

Motion Analysis during Sabot Opening Process

R.S. Acharya¹ & S.D. Naik²

¹VIIIT, Pune-411 048

²Defence Institute of Advanced Technology, Pune-411 025

ABSTRACT

For FSAPDS projectile, the trajectory and stability are dependent on different forces in different phases of the motion. During the first phase gravity, aerodynamic drag along with propellant gas force affect the motion. The motion is influenced by shock wave and mechanical force in sabot opening phase and the effect of time lag during opening of sabots also forms part of this work.

Keywords: Sabot opening process, motion analysis, FSAPDS projectiles

NOMENCLATURE

I_{xx}, I_{yy}, I_{zz}	Moment of inertia about the X, Y, and Z-axis, respectively	l	Projectile characteristics length
m	Mass of projectile	p	Axial spin of the projectile
r	Position vector	x, y, z	Range, altitude, and drift, respectively
V	Velocity of projectile	$C_{L\alpha}/C_{N\alpha}$	Lift/Normal coefficient
C	Mass centre of the projectile body	F_1/M_1	Propellant gas force/moment
Ω	Angular velocity	C_D/C_X	Drag/axial coefficient
C_i	Mass centre of the i^{th} sabot component	F_2/M_2	Aerodynamic force/moment
S	Projectile reference area	$C_{M\alpha}$	Overturning moment
$O-XYZ$	Inertial coordinate system	F_3/M_3	Gravity force/moment coefficient
P	Pressure in gas flow	$C_{Np\alpha}$	Magnus force coefficient
ρ_s	Density of the gas in the vicinity of sabot	$C_{MP\alpha}$	Magnus moment coefficient
ρ	Air density	C_{tp}	Spin damping moment coefficient
		C_{Mqt}	Pitch damping moment coefficient
		C_{Nqt}	Pitch damping force coefficient

C_v	Specific heat of gases around projectile
u, v, w	Velocity components in projectile frame
L_c	Length between the centre and tip of sabot
L_s	Length of the sabot
Φ	Angle of side slip
θ	Angle of attack
$\omega_1, \omega_2, \omega_3$	Angular velocity components of projectile
δ_1, δ_2	Angles made by projectile axis in velocity frame
η_1, η_2	Angles made by the propellant gas direction in projectile frame
$\varepsilon_1, \varepsilon_2$	Angles made by propellant gas direction in inertial frame

Suffixes

1	for the projectile coordinate systems
2	for the velocity coordinate systems
3	for the sabot component-fixed coordinate systems
s	for the sabot
p	for the projectile

Conventions

X	Vector cross product
-----	----------------------

1. INTRODUCTION

The motion of a FSAPDS projectile as it exits from the muzzle end is divided into four phases and two transition periods¹. The propellant gases following the projectile, exert pressure on the projectile and affect its trajectory and stability. The effect of these forces has been discussed in the earlier work by the authors².

The sabots start opening up due to the air flow between the projectile and the sabots. This part of

motion includes the opening process of sabots along with the projectile motion, which is phase II. Opening of sabot components give rise to shock wave. It also develops a mechanical force which acts on the projectile as well as on each sabot component. The shock wave force and mechanical force are the two additional forces to be considered during this motion of the projectile. The openings of sabots generate associated moments relative to projectile. It affects the stability of the projectile.

The motion in this phase has been studied in 6 DOFs with the reduced propellant gas pressure force, aerodynamic forces, and gravity force along with these two additional forces. The trajectory is defined with projectile motion and relative motion of sabot components. The study of the effect of these forces on the trajectory and stability is the aim of this paper.

Each of the sabot components opens up separately. The initial conditions are defined at the end of phase I. Initially, the analysis has been done assuming that all the three sabots start opening at the same instant. The effect of time delay in this opening process of sabot on stability is also included as a part of this study.

2. EQUATIONS OF MOTION OF PROJECTILE

2.1 Forces

Two additional coordinate systems and transformations are required to study the motion, as below (Fig. 1).

- (i) Projectile-fixed coordinate system $C-X_{ii} Y_{ii} Z_{ii}$ (relative to initial position of the i^{th} sabot, $i = 1,2,3$). The initial position of sabot lies in the plane $X_{ii} Y_{ii}$.

C	Centre of mass of the projectile
CX_{ii}	Along projectile direction
CY_{ii}	Vertical axis normal to the CX_{ii}
CZ_{ii}	Completes the right handed system

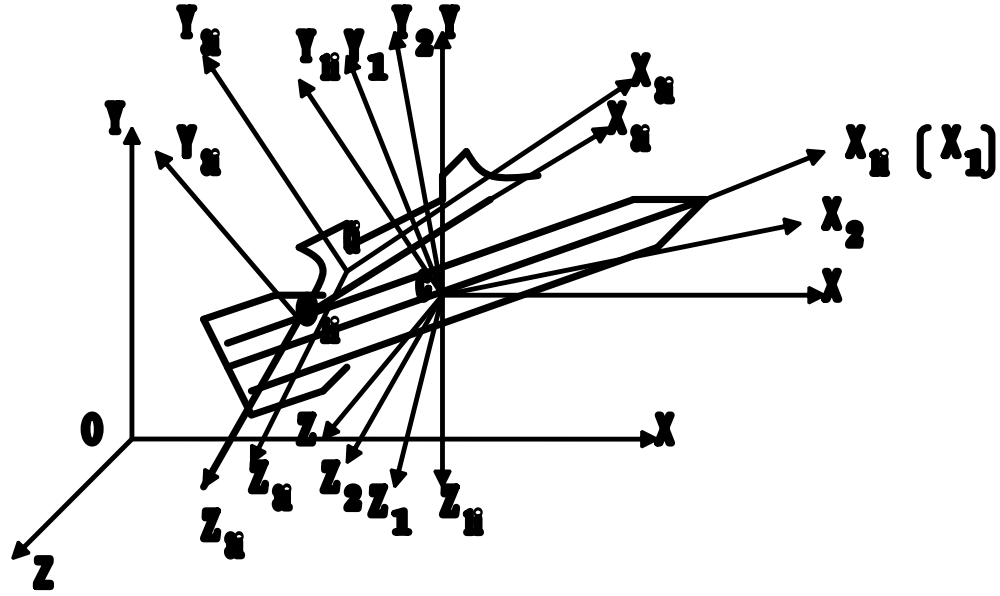


Figure 1. Coordinate system and their interrelationship.

(ii) Sabot component-fixed coordinate system O_{li} -
 $X_{3i} Y_{3i} Z_{3i}$

- O_{li} Tip of i^{th} sabot component
- $O_{li} X_{3i}$ Along sabot direction
- $O_{li} Y_{3i}$ Vertical axis normal to the $O_{li} X_{3i}$
- $O_{li} X_{3i} O_{li} Z_{3i}$ Completes the right handed system.

The corresponding transformations are:

(i) The sabot coordinate system to the projectile-fixed coordinate system

$$(\hat{i}_{3i}, \hat{j}_{3i}, \hat{k}_{3i}) = A^z(\theta_{3i})(\hat{i}_{li}, \hat{j}_{li}, \hat{k}_{li})$$

$$\begin{bmatrix} \hat{i}_{3i} \\ \hat{j}_{3i} \\ \hat{k}_{3i} \end{bmatrix} = A^z(\theta_{3i}) \begin{bmatrix} \hat{i}_{li} \\ \hat{j}_{li} \\ \hat{k}_{li} \end{bmatrix} = \begin{bmatrix} \cos \theta_{3i} & \sin \theta_{3i} & 0 \\ -\sin \theta_{3i} & \cos \theta_{3i} & 0 \\ 0 & 0 & 1 \end{bmatrix} \begin{bmatrix} \hat{i}_{li} \\ \hat{j}_{li} \\ \hat{k}_{li} \end{bmatrix} \quad (1)$$

where θ_{3i} is the angle between the sabot and projectile (Fig. 2).

(ii) The projectile-moving coordinate system to the projectile-fixed coordinate system.

$$(\hat{i}_1, \hat{j}_1, \hat{k}_1) = A^x(\theta_i)(\hat{i}_{1i}, \hat{j}_{1i}, \hat{k}_{1i})$$

$$\begin{bmatrix} \hat{i}_1 \\ \hat{j}_1 \\ \hat{k}_1 \end{bmatrix} = \begin{bmatrix} 1 & 0 & 0 \\ 0 & \cos \theta_i & \sin \theta_i \\ 0 & -\sin \theta_i & \cos \theta_i \end{bmatrix} \begin{bmatrix} \hat{i}_{1i} \\ \hat{j}_{1i} \\ \hat{k}_{1i} \end{bmatrix} \quad (2)$$

where θ_i is the angle between the projectile-moving coordinate system and the projectile-fixed coordinate system.

The propellant gas force, aerodynamic force, and gravity force acting on the projectile are similar to those in phase I². The additional forces due to the sabot opening process are discussed here.

2.1.1 Model for Mechanical Force F_3

The sabots start opening up from the projectile at the tip. This angular motion is due to the air passing between the projectile and the sabot. The

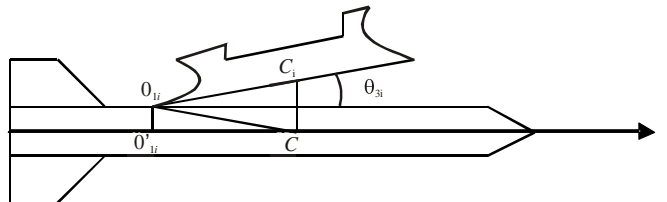


Figure 2. Mass centre of the projectile and sabot.

mechanical force due to this motion can be modelled using spring mass system³. The total mechanical force acting on the projectile is the sum of mechanical forces due to the sabot components.

For three sabot components, it is

$$\overline{F}_3 = \sum_{i=1}^3 \overline{F}_{3i}$$

Due to i^{th} sabot component, the mechanical force along the sabot for a displacement \overline{x} is

$$\overline{F}_{3i} = -K\overline{x} = -K\overline{O_{1i}C_i} = -KL_c\hat{i}_{3i}$$

The mechanical force in projectile-fixed frame becomes

$$\overline{F}_{3i} = -KL_c(\cos\theta_{3i}\hat{i}_{1i} + \sin\theta_{3i}\hat{j}_{1i}) \quad (3)$$

2.1.2 Model for the Shock Wave Force F_4

A shock wave force is generated due to each sabot component. The total shock wave force is the sum of all the corresponding forces.

$$\overline{F}_4 = \sum \overline{F}_{4i}$$

A shock wave force \overline{F}_{4i} is due to pressure and is given by $\overline{F}_{4i} = \text{pressure} \times \text{area}$

The area on which the pressure acts is taken as $1/3^{\text{rd}}$ perimeter of projectile multiplied with the total length of the sabot as the design of the projectile consists of total three sabots.

$$\text{Therefore, area} = \pi (D/3)L_s$$

The pressure is due to air as well as the propellant gases. It can be expressed with the

Bernoulli's pressure as

$$\overline{P}_s = (1/2)\rho_s(\overline{V}_p + \overline{V}_s)^2 \quad (4)$$

Using the equation of the state and the gas law, ρ_s can be approximated to

$$\rho_s = \frac{P}{C_v(\gamma - 1)} \quad (5)$$

The velocity of sabot is due to its angular motion,

$$\overline{V}_s = \overline{\omega} \times \overline{r} \quad \text{where} \quad \overline{\omega} = -\dot{\theta}_{3i}(\hat{i}_{3i} \times \hat{i}_{1i}) \quad (6)$$

From the transformations [Eqn (1)]

$$\overline{\omega} = -\dot{\theta}_{3i} \sin\theta_{3i} \hat{k}_{1i}$$

\overline{r} is position vector along the sabot [Fig. 2].

$$\overline{r} = L_c \hat{i}_{3i} \quad \text{where} \quad L_c = O_{1i}C_i$$

$$= L_c(\cos\theta_{3i}\hat{i}_{1i} + L_c \sin\theta_{3i}\hat{j}_{1i})$$

$$\overline{V}_s = L_c \dot{\theta}_{3i} \sin^2\theta_{3i} \hat{i}_{1i} - L_c \dot{\theta}_{3i} \sin\theta_{3i} \cos\theta_{3i} \hat{j}_{1i} \quad (7)$$

Therefore,

Total velocity

$$\begin{aligned} &= \overline{V}_p + \overline{V}_s \\ &= (\overline{V}_p + L_c \dot{\theta}_{3i} \sin^2\theta_{3i}) \hat{i}_{1i} - L_c \dot{\theta}_{3i} \sin\theta_{3i} \cos\theta_{3i} \hat{j}_{1i} \end{aligned}$$

Pressure

$$\begin{aligned} &= P_s = (1/2)\rho_s(\overline{V}_p + \overline{V}_s)^2 \\ &= (1/2)\rho_s |\overline{V}_p + \overline{V}_s| (\overline{V}_p + \overline{V}_s) \\ &= (1/2)\rho_s V_p (\overline{V}_p + \overline{V}_s) \quad [:\cdot |\overline{V}_p + \overline{V}_s| \equiv V_p] \\ &= (1/2)\rho_s V_p [(V_p + L_c \dot{\theta}_{3i} \sin^2\theta_{3i}) \hat{i}_{1i} \\ &\quad - L_c \dot{\theta}_{3i} \sin\theta_{3i} \cos\theta_{3i} \hat{j}_{1i}] \end{aligned} \quad (8)$$

From the Eqns (2) and (8) shock wave force becomes

$$\begin{aligned} \overline{F}_{4i} &= (1/2)\rho_s V_p \pi (D/3) L_s [(V_p + \\ &\quad L_c \dot{\theta}_{3i} \sin^2\theta_{3i}) \hat{i}_{1i} - L_c \dot{\theta}_{3i} \sin\theta_{3i} \cos\theta_{3i} \hat{j}_{1i}] \end{aligned} \quad (9)$$

2.2 Associated Moments

The mechanical and shock wave forces generate the corresponding moments as

Mechanical force moment

$$\begin{aligned} \overline{M}_{c3} &= [\sqrt{(L_m)^2 - (d/2)^2}] \hat{i}_{1i} \times \overline{F}_3 \\ &\quad [\text{where } L_m = \overline{O_{1i}C}] \end{aligned} \quad (10)$$

Shock wave force moment

$$\overline{M}_{c4} = \overline{r}_1 \times \overline{F}_4 \quad (11)$$

3. 6-DOF EQUATIONS FOR PROJECTILE

In the second phase of motion, the trajectory of the projectile in 6-DOF can be obtained with all these five forces. The force and moment equations are resolved in velocity and projectile coordinate system respectively. The scalar equations are:

$$\begin{aligned} \dot{V}_p = \{ & PA(\cos \varepsilon_1 \cos \varepsilon_2 \cos \theta_2 \cos \phi_2 - \\ & \sin \varepsilon_1 \cos \varepsilon_2 \sin \theta_2 - \sin \varepsilon_2 \cos \theta_2 \sin \phi_2) \\ & + (1/2)\rho SV_p^2[-C_D + (l/V_p)C_{Nqt}[\sin \delta_1 \\ & (-\dot{\phi}_1 \sin \gamma_1 \cos \theta_1 + \dot{\theta}_1 \cos \gamma_1) \\ & + \cos \delta_1 \sin \delta_2(\dot{\phi}_1 \cos \gamma_1 \cos \theta_1 + \dot{\theta}_1 \sin \gamma_1)] \\ & - 3K L_c \cos \theta_{3i} \cos \delta_1 \cos \delta_2 \\ & + (3/2)\rho_S V_p \pi (D/3) L_s (V_p + L_c \dot{\theta}_{3i} \sin^2 \theta_{3i}) \\ & \cos \delta_1 \cos \delta_2 - mg \sin \theta_2\} / (m) \end{aligned} \quad (12)$$

$$\begin{aligned} \dot{\phi}_2 = \{ & PA(\cos \varepsilon_1 \cos \varepsilon_2 \sin \phi_2 + \sin \varepsilon_2 \cos \phi_2) + \\ & (1/2)\rho SV_p^2[-C_{L\alpha} \sin \delta_1 \cos \delta_2 - (pl/V_p)C_{Np\alpha} \sin \delta_2 \\ & + (l/V_p)C_{Nqt}[\cos \delta_1(-\dot{\phi}_1 \sin \gamma_1 \cos \theta_1 + \dot{\theta}_1 \cos \gamma_1) \\ & - \sin \delta_1 \sin \delta_2(\dot{\phi}_1 \cos \gamma_1 \cos \theta_1 + \dot{\theta}_1 \sin \gamma_1)] \\ & + 3K L_c \cos \theta_{3i} \sin \delta_1 \cos \delta_2 \\ & - (3/2)\rho_S V_p \pi (D/3) L_s (V_p + L_c \dot{\theta}_{3i} \sin^2 \theta_{3i}) \\ & \sin \delta_1 \cos \delta_2\} / (-mV_p \cos \theta_2) \end{aligned} \quad (13)$$

$$\begin{aligned} \dot{\theta}_2 = \{ & PA(\cos \varepsilon_1 \cos \varepsilon_2 \sin \theta_2 \cos \phi_2 + \\ & \sin \varepsilon_1 \cos \varepsilon_2 \cos \theta_2 - \sin \varepsilon_2 \sin \theta_2 \sin \phi_2) \\ & + (1/2)\rho_S SV_p^2[C_{L\alpha} \sin \delta_2 - \\ & (pl/V_p)C_{Np\alpha} \sin \delta_1 \cos \delta_2 - (l/V_p)C_{Nqt} \\ & \cos \delta_2(\dot{\phi}_1 \cos \gamma_1 \cos \theta_1 + \dot{\theta}_1 \sin \gamma_1)] - \\ & 3K L_c \cos \theta_{3i} \sin \delta_2 + (3/2)\rho_S V_p \pi (D/3) \\ & L_s (V_p + L_c \dot{\theta}_{3i} \sin^2 \theta_{3i}) \sin \delta_2 + mg \cos \theta_2\} / (mV_p) \end{aligned} \quad (14)$$

Moments equations are:

$$\begin{aligned} I_{xx}(\partial/\partial t)(\dot{\phi}_1 \sin \theta_1 + \dot{\gamma}_1) = & r_p PA(-\sin \eta_1 \cos \eta_2 \sin \varepsilon_2 \\ & + \sin \eta_2 \sin \varepsilon_1 \cos \varepsilon_2) + (1/2)\rho SV_p^2 l C_{tp}(pl/V_p) \end{aligned} \quad (15)$$

$$\begin{aligned} I_{YY}(\partial/\partial t)(\dot{\phi}_1 \cos \gamma_1 \cos \theta_1 + \dot{\theta}_1 \sin \gamma_1) + (I_{xx} - I_{YY}) \\ (\dot{\phi}_1 \sin \theta_1 + \dot{\gamma}_1)(-\dot{\phi}_1 \sin \gamma_1 \cos \theta_1 + \dot{\theta}_1 \cos \gamma_1) \\ = r_p PA(\sin \eta_2 \cos \varepsilon_1 \cos \varepsilon_2 - \cos \eta_1 \cos \eta_2 \sin \varepsilon_2) \\ + (1/2)\rho SV_p^2 l [-C_{M\alpha} \cos \delta_1 \sin \delta_2 + C_{Map}(pl/V_p) \sin \delta_1 \\ + (l/V_p)(C_{Mqt})(\dot{\phi}_1 \cos \gamma_1 \cos \theta_1 + \dot{\theta}_1 \sin \gamma_1)] \end{aligned} \quad (16)$$

$$\begin{aligned} [I_{ZZ}(\partial/\partial t)(-\dot{\phi}_1 \sin \gamma_1 \cos \theta_1 + \dot{\theta}_1 \cos \gamma_1) \\ + (I_{YY} - I_{xx})(\dot{\phi}_1 \sin \theta_1 + \dot{\gamma}_1)(\dot{\phi}_1 \cos \gamma_1 \cos \theta_1 \\ + \dot{\theta}_1 \sin \gamma_1)] \\ = r_p PA(-\cos \eta_1 \cos \eta_2 \sin \varepsilon_1 \cos \varepsilon_2 + \sin \eta_1 \cos \eta_2 \\ \cos \varepsilon_1 \cos \varepsilon_2) + (1/2)\rho SV_p^2 l [-C_{M\alpha} \sin \delta_1 + \\ C_{Map}(pl/V_p) \cos \delta_1 \sin \delta_2 + (l/V_p)(C_{Mqt}) \\ (-\dot{\phi}_1 \sin \gamma_1 \cos \theta_1 + \dot{\theta}_1 \cos \gamma_1)] \end{aligned} \quad (17)$$

The velocity in inertial frame is

$$\dot{x} = V_p \cos \theta_2 \cos \phi_2 \quad (18)$$

$$\dot{y} = V_p \sin \theta_2 \cos \phi_2 \quad (19)$$

$$\dot{z} = -V_p \sin \phi_2 \quad (20)$$

4. EQUATIONS OF MOTION FOR SABOT COMPONENTS

The sabot components move relative to the projectile body. The relative motion can be studied with the help of moment equations. The influence factor should involve the mechanical action and shock wave action. The motion equations of each sabot component will be established in the projectile fixed coordinate system.

4.1 Total Acceleration of the i^{th} Component: Sabot

Total acceleration of the i^{th} sabot component \bar{a}_i consists of sabot acceleration relative to the projectile and projectile acceleration due to \bar{V}_p . Thus, \bar{a}_i is given by

$$\bar{a}_i = \bar{a}_{ir} + \frac{d\bar{V}}{dt} \quad \because \bar{V} = \dot{\bar{r}} + \bar{\Omega}_1 X \bar{r} \quad (21)$$

$$\begin{aligned} &= \bar{a}_{ir} + [\dot{\bar{r}} + \frac{\partial \bar{\Omega}_1}{\partial t} X \bar{r} + \bar{\Omega}_1 X (\bar{\Omega}_1 X \bar{r})] + [2\bar{\Omega}_1 X \dot{\bar{r}}] \\ &= \bar{a}_{ir} + \bar{a}_{ie} + \bar{a}_{ik} \end{aligned} \quad (22)$$

where $\bar{a}_{ir}, \bar{a}_{ie}, \bar{a}_{ik}$ denote the relative acceleration, transport acceleration and coriolis acceleration of the i^{th} sabot component relative to the projectile body, respectively.

The contribution from these accelerations can be compared. It was observed that the contribution from coriolis acceleration is very small in comparison with relative and transport acceleration in this short interval of time, and hence, can be ignored. The remaining two terms are considered here to get the set of equations.

4.1.1 Relative Acceleration

The acceleration vector \bar{a}_{ir} of the i^{th} sabot component relative to the projectile from Eqns (1) and (2) is given by

$$\bar{a}_{ir} = \frac{d\bar{\omega}_{is}}{dt} X \bar{r}_i + \bar{\omega}_{is} X \bar{V}_{is} \quad (23)$$

$$\begin{aligned} &= -L_c [\ddot{\theta}_{3i} \sin \theta_{3i} + (\dot{\theta}_{3i})^2 \cos \theta_{3i}] \hat{i}_{1i} \\ &+ L_c [\ddot{\theta}_{3i} \cos \theta_{3i} - (\dot{\theta}_{3i})^2 \sin \theta_{3i}] \hat{j}_{1i} \end{aligned} \quad (24)$$

4.1.2 Acceleration of Transport

Transport acceleration of the i^{th} sabot component

$$\bar{a}_{ie} = \ddot{\bar{r}} + \frac{\partial \bar{\Omega}_1}{\partial t} X \bar{r} + \bar{\Omega}_1 X (\bar{\Omega}_1 X \bar{r})$$

The linear acceleration of the projectile is

$$\begin{aligned} \ddot{\bar{r}} = \dot{V}_p &[\cos \delta_1 \cos \delta_2 \hat{i}_{1i} + (\sin \delta_1 \cos \gamma_i + \\ &\cos \delta_1 \sin \delta_2 \sin \gamma_i) \hat{j}_{1i} + (\sin \delta_1 \sin \gamma_i - \\ &\cos \delta_1 \sin \delta_2 \cos \gamma_i) \hat{k}_{1i}] \end{aligned} \quad (25)$$

$\bar{\Omega}_1$ is the angular acceleration of the projectile coordinate system.

$$\begin{aligned} \bar{\Omega}_1 &= (\dot{\phi}_1 \sin \theta_1 + \dot{\gamma}_1) \hat{i}_1 \\ &+ (\dot{\phi}_1 \cos \gamma_1 \cos \theta_1 + \dot{\theta}_1 \sin \gamma_1) \hat{j}_1 \\ &+ (-\dot{\phi}_1 \sin \gamma_1 \cos \theta_1 + \dot{\theta}_1 \cos \gamma_1) \hat{k}_1 \end{aligned} \quad (26)$$

Using the transformations (1)

$$\bar{\Omega}_1 = (\dot{\gamma}_1 + \dot{\phi}_1 \sin \theta_1) \hat{i}_{1i} + \dot{\phi}_1 \cos \theta_1 \hat{j}_{1i} + \dot{\theta}_1 \hat{k}_{1i} \quad (27)$$

$$\begin{aligned} \frac{\partial \bar{\Omega}_1}{\partial t} X \overline{CC_i} &= -\frac{\partial \dot{\theta}_1}{\partial t} (L_c \sin \theta_{3i} + \frac{l}{2}) \hat{i}_{1i} + \frac{\partial \dot{\theta}_1}{\partial t} \\ &(L_c \cos \theta_{3i} - L_m) \hat{j}_{1i} + [\frac{\partial (\dot{\gamma}_1 + \dot{\phi}_1 \sin \theta_1)}{\partial t} \\ &(L_c \sin \theta_{3i} + \frac{l}{2}) + \frac{\partial (\dot{\phi}_1 \cos \theta_1)}{\partial t} (L_c \cos \theta_{3i} - L_m)] \hat{k}_{1i} \end{aligned} \quad (28)$$

$$\begin{aligned} &\bar{\Omega}_1 X (\bar{\Omega}_1 X \overline{CC_i}) \\ &= [(\dot{\gamma}_1 \dot{\phi}_1 \cos \theta_1 + \dot{\phi}_1^2 \cos \theta_1 \sin \theta_1) (L_c \sin \theta_{3i} + \frac{l}{2}) \\ &- \dot{\phi}_1^2 \cos^2 \theta_1 (L_c \cos \theta_{3i} - L_m) - \dot{\theta}_1^2 (L_c \cos \theta_{3i} - L_m)] \hat{i}_{1i} \\ &+ [-\dot{\theta}_1^2 (L_c \sin \theta_{3i} + \frac{l}{2}) - (\dot{\gamma}_1 + \dot{\phi}_1 \sin \theta_1)^2 (L_c \sin \theta_{3i} + \frac{l}{2}) \\ &+ (\dot{\gamma}_1 + \dot{\phi}_1 \sin \theta_1) \dot{\phi}_1 \cos \theta_1 (L_c \cos \theta_{3i} - L_m)] \hat{j}_{1i} \\ &+ [\dot{\theta}_1 (\dot{\gamma}_1 + \dot{\phi}_1 \sin \theta_1) (L_c \cos \theta_{3i} - L_m) \\ &+ \dot{\phi}_1 \dot{\theta}_1 \cos \theta_1 (L_c \sin \theta_{3i} + \frac{l}{2})] \hat{k}_{1i} \end{aligned} \quad (29)$$

From the Eqns (25), (28) and (29)

$$\begin{aligned} \bar{a}_{ie} &= \ddot{\bar{r}} + \frac{\partial \bar{\Omega}_1}{\partial t} X \overline{CC_i} + \bar{\Omega}_1 X (\bar{\Omega}_1 X \overline{CC_i}) \\ &= [\dot{V}_p \cos \delta_1 \cos \delta_2 - \frac{\partial \dot{\theta}_1}{\partial t} (L_c \sin \theta_{3i} + \frac{l}{2}) + (\dot{\gamma}_1 \dot{\phi}_1 \cos \theta_1 \\ &+ \dot{\phi}_1^2 \cos \theta_1 \sin \theta_1) (L_c \sin \theta_{3i} + \frac{l}{2}) - \dot{\phi}_1^2 \cos^2 \theta_1 \\ &(L_c \cos \theta_{3i} - L_m) - \dot{\theta}_1^2 (L_c \cos \theta_{3i} - L_m)] \hat{i}_{1i} \\ &+ [\dot{V}_p (\sin \delta_1 \cos \gamma_i + \cos \delta_1 \sin \delta_2 \sin \gamma_i) \\ &+ \frac{\partial \dot{\theta}_1}{\partial t} (L_c \cos \theta_{3i} - L_m) - \dot{\theta}_1^2 (L_c \sin \theta_{3i} + \frac{l}{2}) \end{aligned}$$

$$\begin{aligned}
 & -(\dot{\gamma}_1 + \dot{\phi}_1 \sin \theta_1)^2 (L_c \sin \theta_{3i} + \frac{l}{2}) + (\dot{\gamma}_1 + \dot{\phi}_1 \sin \theta_1) \\
 & \quad \dot{\phi}_1 \cos \theta_1 (L_c \cos \theta_{3i} - L_m) \hat{j}_{1i} + [\dot{V}_p (\sin \delta_1 \sin \gamma_i \\
 & - \cos \delta_1 \sin \delta_2 \cos \gamma_i) + \frac{\partial(\dot{\gamma}_1 + \dot{\phi}_1 \sin \theta_1)}{\partial t} \\
 & \quad (L_c \sin \theta_{3i} + \frac{l}{2}) + \frac{\partial(\dot{\phi}_1 \cos \theta_1)}{\partial t} (L_c \cos \theta_{3i} - L_m) \\
 & + \dot{\theta}_1 (\dot{\gamma}_1 + \dot{\phi}_1 \sin \theta_1) (L_c \cos \theta_{3i} - L_m) \\
 & + \dot{\phi}_1 \dot{\theta}_1 \cos \theta_1 (L_c \sin \theta_{3i} + \frac{l}{2}) \hat{k}_{1i} \quad (30)
 \end{aligned}$$

From the eqns (24), (30), the total acceleration \bar{a}_i is given by

$$\begin{aligned}
 \bar{a}_i &= \bar{a}_{ir} + \bar{a}_{ie} \\
 &= \{-L_c [\ddot{\theta}_{3i} \sin \theta_{3i} + (\dot{\theta}_{3i})^2 \cos \theta_{3i}] \\
 & \quad + \dot{V}_p \cos \delta_1 \cos \delta_2 - \frac{\partial \dot{\theta}_1}{\partial t} (L_c \sin \theta_{3i} + \frac{l}{2}) \\
 & \quad + (\dot{\gamma}_1 \dot{\phi}_1 \cos \theta_1 + \dot{\phi}_1^2 \cos \theta_1 \sin \theta_1) (L_c \sin \theta_{3i} + \frac{l}{2}) \\
 & \quad - \dot{\phi}_1^2 \cos^2 \theta_1 (L_c \cos \theta_{3i} - L_m) - \dot{\theta}_1^2 (L_c \cos \theta_{3i} \\
 & \quad - L_m) \hat{i}_{1i} + \{L_c [\ddot{\theta}_{3i} \cos \theta_{3i} - (\dot{\theta}_{3i})^2 \sin \theta_{3i}] \\
 & \quad + \dot{V}_p (\sin \delta_1 \cos \gamma_i + \cos \delta_1 \sin \delta_2 \sin \gamma_i) \\
 & \quad + \frac{\partial \dot{\theta}_1}{\partial t} (L_c \cos \theta_{3i} - L_m) - \dot{\theta}_1^2 (L_c \sin \theta_{3i} + \frac{l}{2}) \\
 & \quad - (\dot{\gamma}_1 + \dot{\phi}_1 \sin \theta_1)^2 (L_c \sin \theta_{3i} + \frac{l}{2}) \\
 & \quad + (\dot{\gamma}_1 + \dot{\phi}_1 \sin \theta_1) \dot{\phi}_1 \cos \theta_1 (L_c \cos \theta_{3i} - L_m) \hat{j}_{1i} \\
 & \quad + \{\dot{V}_p (\sin \delta_1 \sin \gamma_i - \cos \delta_1 \sin \delta_2 \cos \gamma_i) \\
 & \quad + \frac{\partial(\dot{\gamma}_1 + \dot{\phi}_1 \sin \theta_1)}{\partial t} (L_c \sin \theta_{3i} + \frac{l}{2}) + \frac{\partial(\dot{\phi}_1 \cos \theta_1)}{\partial t} \\
 & \quad (L_c \cos \theta_{3i} - L_m) + \dot{\theta}_1 (\dot{\gamma}_1 + \dot{\phi}_1 \sin \theta_1) (L_c \cos \theta_{3i} - L_m) \\
 & \quad + \dot{\phi}_1 \dot{\theta}_1 \cos \theta_1 (L_c \sin \theta_{3i} + \frac{l}{2}) \hat{k}_{1i} \quad (31)
 \end{aligned}$$

4.2 Force Equations of Sabot

The force equations of the sabot are resolved in projectile-fixed coordinate system. Different forces are as follows:

$$\sum \bar{F}_s = \bar{F}_{1s} + \bar{F}_{2s} + \bar{F}_{3s} + \bar{F}_{4s} + \bar{F}_{5s}$$

where \bar{F}_{1s} is the propellant gas force, \bar{F}_{2s} is the aerodynamic force, \bar{F}_{3s} is the mechanical force, \bar{F}_{4s} is the shockwave force, and \bar{F}_{5s} is the gravity force.

$$\begin{aligned}
 \bar{F}_s &= \{PA \cos \eta_1 \cos \eta_2 + (1/2) \rho S_s u^2 C_{xs} \\
 & \quad - K L_c \cos \theta_{3i} - 3P_m \pi (Ds/2) L_s - m_s g \sin \theta_1 \hat{i}_{1i} \\
 & \quad + \{-PA (\sin \eta_1 \cos \eta_2 \cos \gamma_i + \sin \eta_2 \sin \gamma_i) \\
 & \quad + (1/2) \rho S_s u^2 (l_s/u) C_{Nqs} (\dot{\theta}_1 \cos \gamma_i + \dot{\phi}_1 \cos \theta_1 \sin \gamma_i) \\
 & \quad - K L_c \sin \theta_{3i} - m_s g \cos \gamma_{1i} \cos \theta_1 \hat{j}_{1i} \\
 & \quad + \{PA (-\sin \eta_1 \cos \eta_2 \sin \gamma_i + \sin \eta_2 \cos \gamma_i) \\
 & \quad + (1/2) \rho S_s u^2 (l_s/u) C_{Nqs} (\dot{\theta}_1 \sin \gamma_i - \dot{\phi}_1 \cos \theta_1 \cos \gamma_i) \\
 & \quad + m_s g \sin \gamma_i \cos \theta_1 \hat{k}_{1i} \quad (32)
 \end{aligned}$$

The dynamic vector equations of the centre motion of all sabot components are obtained as

$$m(\bar{a}_{ir} + \bar{a}_{ie} + \bar{a}_{ik}) = \sum \bar{F}_s = \bar{F}_{1s} + \bar{F}_{2s} + \bar{F}_{3s} + \bar{F}_{4s} + \bar{F}_{5s} \quad (33)$$

From the Eqns (31) to (33), the relative scalar equations of the sabot are

$$\begin{aligned}
 & PA \cos \eta_1 \cos \eta_2 + (1/2) \rho S_s u^2 C_{xs} - K L_c \cos \theta_{3i} \\
 & - 3P_m \pi (Ds/2) L_s - m_s g \sin \theta_1 \\
 & = -L_c [\ddot{\theta}_{3i} \sin \theta_{3i} + (\dot{\theta}_{3i})^2 \cos \theta_{3i}] + \dot{V}_p \cos \delta_1 \cos \delta_2 \\
 & - \frac{\partial \dot{\theta}_1}{\partial t} (L_c \sin \theta_{3i} + \frac{l}{2}) + (\dot{\gamma}_1 \dot{\phi}_1 \cos \theta_1 + \dot{\phi}_1^2 \cos \theta_1 \sin \theta_1) \\
 & \quad (L_c \sin \theta_{3i} + \frac{l}{2}) - \dot{\phi}_1^2 \cos^2 \theta_1 (L_c \cos \theta_{3i} - L_m) \\
 & - \dot{\theta}_1^2 (L_c \cos \theta_{3i} - L_m) \quad (34) \\
 & - PA (\sin \eta_1 \cos \eta_2 \cos \gamma_i + \sin \eta_2 \sin \gamma_i) + \\
 & (1/2) \rho S_s u^2 (l_s/u) C_{Nqs} (\dot{\theta}_1 \cos \gamma_i + \dot{\phi}_1 \cos \theta_1 \sin \gamma_i) \\
 & - K L_c \sin \theta_{3i} - m_s g \cos \gamma_{1i} \cos \theta_1 \\
 & = L_c [\ddot{\theta}_{3i} \cos \theta_{3i} - (\dot{\theta}_{3i})^2 \sin \theta_{3i}] + \dot{V}_p (\sin \delta_1 \cos \gamma_i \\
 & + \cos \delta_1 \sin \delta_2 \sin \gamma_i)
 \end{aligned}$$

$$\begin{aligned}
 & + \frac{\partial \dot{\theta}_1}{\partial t} (L_c \cos \theta_{3i} - L_m) - \dot{\theta}_1^2 (L_c \sin \theta_{3i} + \frac{l}{2}) \\
 & - (\dot{\gamma}_1 + \dot{\phi}_1 \sin \theta_1)^2 (L_c \sin \theta_{3i} + \frac{l}{2}) + (\dot{\gamma}_1 + \dot{\phi}_1 \sin \theta_1) \\
 & \dot{\phi}_1 \cos \theta_1 (L_c \cos \theta_{3i} - L_m) \tag{35}
 \end{aligned}$$

$$\begin{aligned}
 & PA(-\sin \eta_1 \cos \eta_2 \sin \gamma_i + \sin \eta_2 \cos \gamma_i) + \\
 & (1/2)\rho S_s u^2 (l_s / u) C_{Nqs} \\
 & (\dot{\theta}_1 \sin \gamma_i - \dot{\phi}_1 \cos \theta_1 \cos \gamma_i) + m_s g \sin \gamma_i \cos \theta_1 \\
 & = \dot{V}_p (\sin \delta_1 \sin \gamma_i - \cos \delta_1 \sin \delta_2 \cos \gamma_i) + \\
 & \frac{\partial (\dot{\gamma}_1 + \dot{\phi}_1 \sin \theta_1)}{\partial t} (L_c \sin \theta_{3i} + \frac{l}{2}) + \frac{\partial (\dot{\phi}_1 \cos \theta_1)}{\partial t} \\
 & (L_c \cos \theta_{3i} - L_m) + \dot{\theta}_1 (\dot{\gamma}_1 + \dot{\phi}_1 \sin \theta_1) (L_c \cos \theta_{3i} - L_m) \\
 & + \dot{\phi}_1 \dot{\theta}_1 \cos \theta_1 (L_c \sin \theta_{3i} + \frac{l}{2}) \tag{36}
 \end{aligned}$$

4.3 Moment Equations of Sabot

The forces generate moments due to which sabots move relative to projectile. The relative moment equations of sabot component relative to projectile are:

$$\begin{aligned}
 & I_{XXS} \frac{\partial}{\partial t} (\dot{\gamma}_1 + \dot{\phi}_1 \sin \theta_1) \\
 & + \dot{\phi}_1 \cos \theta_1 (I_{ZZS} (\dot{\theta}_1 + \dot{\theta}_{3i}) - \dot{\theta}_1 I_{YYS}) \\
 & = L_c PA \sin \theta_{3i} (-\sin \eta_1 \cos \eta_2 \sin \gamma_i + \sin \eta_2 \cos \gamma_i) \\
 & + m_s \{ [V_p (\sin \delta_1 \cos \gamma_i + \cos \delta_1 \sin \delta_2 \sin \gamma_i) \\
 & + \theta_1 L_m (\dot{\theta}_1 + \dot{\theta}_{3i}) L_c \cos \theta_{3i}] [V_p (\sin \delta_1 \sin \gamma_i \\
 & - \cos \delta_1 \sin \delta_2 \cos \gamma_i) + \frac{l}{2} (\dot{\gamma}_1 + \dot{\phi}_1 \sin \theta_1) \\
 & + \dot{\phi}_1 \cos \theta_1 L_m] - m_s [V_p (\sin \delta_1 \sin \gamma_i - \cos \delta_1 \sin \delta_2 \cos \gamma_i) \\
 & + \frac{l}{2} (\dot{\gamma}_1 + \dot{\phi}_1 \sin \theta_1) + \dot{\phi}_1 \cos \theta_1 L_m \\
 & + (\dot{\gamma}_1 + \dot{\phi}_1 \sin \theta_1) L_c \sin \theta_{3i} - \dot{\phi}_1 \cos \theta_1 L_c \cos \theta_{3i}] \\
 & [V_p (\sin \delta_1 \cos \gamma_i + \cos \delta_1 \sin \delta_2 \sin \gamma_i) + \dot{\theta}_1 L_m] \tag{37}
 \end{aligned}$$

$$\begin{aligned}
 & I_{YYS} \frac{\partial}{\partial t} (\dot{\phi}_1 \cos \theta_1) + (\dot{\gamma}_1 + \dot{\phi}_1 \sin \theta_1) [\dot{\theta}_1 I_{XXS} - I_{ZZS} (\dot{\theta}_1 + \dot{\theta}_{3i})] \\
 & = -L_c PA \cos \theta_{3i} (-\sin \eta_1 \cos \eta_2 \sin \gamma_i + \sin \eta_2 \cos \gamma_i) \\
 & + (1/2)\rho S_s V_p^2 l_s \{ C_{Mpas} (\sin \delta_1 \cos \gamma_i \\
 & - \cos \delta_1 \sin \delta_2 \sin \gamma_i) \\
 & + m_s [V_p (\sin \delta_1 \sin \gamma_i - \cos \delta_1 \sin \delta_2 \cos \gamma_i) \\
 & + \frac{l}{2} (\dot{\gamma}_1 + \dot{\phi}_1 \sin \theta_1) + \dot{\phi}_1 \cos \theta_1 L_m + (\dot{\gamma}_1 + \dot{\phi}_1 \sin \theta_1) \\
 & L_c \sin \theta_{3i} - \dot{\phi}_1 \cos \theta_1 L_c \cos \theta_{3i}] [V_p \cos \delta_1 \cos \delta_2 - \frac{l}{2} \dot{\theta}_1] \\
 & - m_s [V_p \cos \delta_1 \cos \delta_2 - \frac{l}{2} \dot{\theta}_1 - (\dot{\theta}_1 + \dot{\theta}_{3i}) L_c \sin \theta_{3i}] \\
 & [V_p (\sin \delta_1 \sin \gamma_i - \cos \delta_1 \sin \delta_2 \cos \gamma_i) \\
 & + \frac{l}{2} (\dot{\gamma}_1 + \dot{\phi}_1 \sin \theta_1) + \dot{\phi}_1 \cos \theta_1 L_m] \tag{38}
 \end{aligned}$$

$$\begin{aligned}
 & I_{ZZS} \frac{\partial}{\partial t} (\dot{\theta}_1 + \dot{\theta}_{3i}) + I_{YYS} \dot{\phi}_1 \cos \theta_1 (\dot{\gamma}_1 + \dot{\phi}_1 \sin \theta_1 - \dot{\phi}_1 \cos \theta_1) \\
 & = -[L_c PA \cos \theta_{3i} (\sin \eta_1 \cos \eta_2 \cos \gamma_i + \sin \eta_2 \sin \gamma_i) + \\
 & L_c PA \sin \theta_{3i} \cos \eta_1 \cos \eta_2] + (1/2)\rho S_s V_p^2 l_s [C_{Mpas} \\
 & (\sin \delta_1 \sin \gamma_i + \cos \delta_1 \sin \delta_2 \cos \gamma_i) + (l_s / V_p) C_{Mqs} \dot{\theta}_{3i}] \\
 & + 3 (1/2)\rho V_p \pi (D_s/3) L_s (V_p - L_c \dot{\theta}_{3i} \sin^2 \theta_{3i}) L_c \sin \theta_{3i} \\
 & + m_s [V_p \cos \delta_1 \cos \delta_2 - \frac{l}{2} \dot{\theta}_1 - (\dot{\theta}_1 + \dot{\theta}_{3i}) L_c \sin \theta_{3i}] \\
 & [V_p (\sin \delta_1 \cos \gamma_i + \cos \delta_1 \sin \delta_2 \sin \gamma_i) + \dot{\theta}_1 L_m] \\
 & - m_s [V_p (\sin \delta_1 \cos \gamma_i + \cos \delta_1 \sin \delta_2 \sin \gamma_i) + \\
 & \dot{\theta}_1 L_m (\dot{\theta}_1 + \dot{\theta}_{3i}) L_c \cos \theta_{3i}] \\
 & V_p \cos \delta_1 \cos \delta_2 - \frac{l}{2} \dot{\theta}_1] \tag{39}
 \end{aligned}$$

5. SIMULATIONS RESULTS

Equations (12) to (20) and Eqns (44) to (46) give the mathematical model for trajectory of the projectile in phase II. The above equations are solved for values of 18 variables which includes $x, y, z, u, v, w, \theta_1, \theta_2, \theta_{3i}, \Phi_1, \Phi_2, \gamma_1, \theta_1 \text{dot}, \theta_2 \text{dot}, \theta_{3i} \text{dot}, \Phi_1 \text{dot}, \Phi_2 \text{dot}, \gamma_1 \text{dot}$. The trajectory for phase II over the time period 0.001 to 0.002 s has been simulated for the following data with fixed step size $h = 0.0001$ (Fig. 3).

5.1 Data

$P = 46.112 \text{ Mpa}; I_{xx} = 3.66 \text{ kg/m}^3;$
 $\rho = 1.225 \text{ kg/m}^3; I_{yy} = 549.06 \text{ kg/m}^3;$
 $l = 0.486 \text{ m}; m = 6.4 \text{ kg};$
 $p = 145 \text{ rpm}; C_x = 1.25;$
 $C_N = 7.02; C_{Np\alpha} = 0;$
 $C_{Nq\alpha} = 0; C_{ip} = 0;$
 $C_{Mqt} = -570.6; C_{Nq} = 0;$
 $V_p = 1447.9 \text{ m/s}; C_{M\alpha} = 2.5;$
 $\phi_1 = 1.5^\circ; \phi_1 \text{ dot} = .03066^\circ;$
 $\theta_1 = 1.5^\circ; \theta_1 \text{ dot} = -0.3942^\circ;$
 $\theta_{3i} = 0.1^\circ; \theta_3 \text{ dot} = 0.2^\circ;$

$\gamma_1 = 0.5^\circ; \gamma_1 \text{ dot} = 0.3^\circ;$
 $\eta_1 = \eta_2$
 $= \varepsilon_1 = \varepsilon_2 = 0;$
 $x = 1.4489 \text{ m}; y = 0.0023772 \text{ m};$
 $z = -0.0001255; t = 0.001 \text{ s};$
 $D = 0.066 \text{ m}; \rho_s = 71.2 \text{ m};$
 $L_c = 0.3 \text{ m}; L_s = 0.4 \text{ m};$
 $L_m = 0.346 \text{ m}; m_s = 2.8;$
 $I_{xxs} = 0.4 \text{ kg/m}^3; I_{yys} = 560 \text{ kg/m}^3 = I_{zcs};$
 $C_{mps} = -2.6; C_{mqs} = -58$

5.2 Simulations Results

Table. 1 shows the simulation results.

Table 1. Simulation results of the trajectory of projectile in phase II

t	V	x	y	z	$\gamma \text{ 1dot deg}$
0.0010	1447.9	1.4489	0.0023772	-0.00012550	0.2999618
0.0011	1447.7	1.5937	0.0025968	-0.00016928	0.2999618
0.0012	1447.5	1.7385	0.0028108	-0.00021766	0.2999045
0.0013	1447.3	1.8833	0.0030193	-0.00027065	0.2998759
0.0014	1447.0	2.0281	0.0032222	-0.00032825	0.2998472
0.0015	1446.8	2.1728	0.0034196	-0.00039044	0.2998129
0.0016	1446.6	2.3176	0.0036115	-0.00045725	0.2997785
0.0017	1446.4	2.4624	0.0037978	-0.00052866	0.2997441
0.0018	1446.2	2.6072	0.0039785	-0.00060467	0.2991369
0.0019	1446.0	2.7520	0.0041536	-0.00068528	0.2991025
0.0020	1445.8	2.8968	0.0043231	-0.00077050	0.2987588

$\Phi \text{ 2deg}$	$\theta \text{ 2 deg}$	$\Phi \text{ 1deg}$	$\theta \text{ 1deg}$	$\gamma \text{ 1deg}$	$\theta \text{ 3i dot deg}$	$\theta \text{ 3i deg}$
0.0164108	0.0879605	1.1999045	1.499809	0.49993253	0.1999764	0.0999854
0.0182332	0.0857778	1.1998472	1.4997518	0.49993253	0.3370102	0.2370248
0.0200549	0.0835894	1.1998472	1.4997518	0.49993253	0.4742731	0.5117626
0.0218767	0.0814010	1.1998472	1.4996945	0.49993253	0.0611725	0.6494780
0.023699	0.0792069	1.1997899	1.4996372	0.49993253	0.7494462	0.7873711
0.0255208	0.0770070	1.1997327	1.4996372	0.49993253	0.8873966	0.9255506
0.0273426	0.0748071	1.1996754	1.4995799	0.49993253	1.0255188	1.0639020
0.0291644	0.0726015	1.1996181	1.4995226	0.49993253	1.1638701	1.2024825
0.0309861	0.0703959	1.1995035	1.4995226	0.49993253	1.3025080	1.3412922
0.0328073	0.0681846	1.1993889	1.4994653	0.49993253	1.4413176	1.3418651
0.0346285	0.0659733	1.1992171	1.4994653	0.49993253	1.5803565	1.4803310

It was observed that

- The projectile travels a distance of 1.44 m (Fig. 4).
- Velocity decreases by approximate 2.1 m/s (Fig. 3).
- Angle of attack θ_2 decreases but θ_1 remains constant.
- Angles of side slip Φ_2 increases and Φ_1 decreases.
- y increases whereas z decreases but variation is very small. The trajectory in cross plane of the projectile is bounded, and hence remains stable (Fig. 5).
- The projectile slightly drifts away to the left.
- Angle θ_{3i} between sabot and projectile starts increasing and it increases by 1.3803456° with constant rate, due to mechanical and shockwave force (Fig. 6).
- Spin slowly starts decreasing.

6. STABILITY OF MOTION

The stability of the projectile motion in phase I has been discussed with modified stability parameter and it was observed that the motion remains stable due to perturbation caused by pressure gradient and damping moment². The modified stability parameter has been discussed due to shock wave and mechanical forces exerted on the projectile body.

It is assumed that the three sabots start opening simultaneously and exert the same force on the projectile. Hence, the resultant force on the projectile gets added along the projectile axis and the normal components get cancelled.

The equations for stability in projectile-fixed frame are:

$$\begin{aligned} & \left(\frac{\partial u}{\partial t} + \omega_2 w - \omega_3 v\right) \hat{i}_1 + \left(\frac{\partial v}{\partial t} + \omega_3 u - \omega_1 w\right) \hat{j}_1 \\ & + \left(\frac{\partial w}{\partial t} + \omega_1 v - \omega_2 u\right) \hat{k}_1 \\ & = \{PA \cos \eta_1 \cos \eta_2 - (1/2)\rho Su^2 C_D - 3K L_c \cos \theta_{3i} \\ & - mg \sin \theta_1 + (3/2)\rho Vp \pi (D/2) L_s (Vp \\ & + L_c \dot{\theta}_{3i} \sin^2 \theta_{3i})\} \hat{i}_1 + \{-PA \sin \eta_1 \cos \eta_2 \\ & + (1/2)\rho Su^2 [-C_N (v/u) + IC_{Nqt} (\omega_3 / u)] \end{aligned}$$

$$- mg \cos \gamma_1 \cos \theta_1 \} \hat{j}_1 + \{PA \sin \eta_2 - (1/2)\rho Su^2 [(w/u)C_N + IC_{Nqt} (\omega_2 / u)] + mg \sin \gamma_1 \cos \theta_1 \} \hat{k}_1 \quad (40)$$

$$\begin{aligned} & [I_{xx}(\partial/\partial t)\omega_1 + I_{YY}\omega_2\omega_3 - I_{YY}\omega_3\omega_2] \hat{i}_1 + \\ & [I_{YY}(\partial/\partial t)\omega_2 + I_{xx}\omega_3\omega_1 - I_{YY}\omega_1\omega_3] \hat{j}_1 \\ & + [I_{YY}(\partial/\partial t)\omega_3 + I_{YY}\omega_1\omega_2 - I_{xx}\omega_2\omega_1] \hat{k}_1 \\ & = (1/2)\rho SC_{ip}u^2 l(pl/u)\hat{i}_1 + \{(1/2)\rho Su^2 l [(w/u)C_{M\alpha} \\ & + C_{M\alpha p}(pl/V_p)(v/u) + IC_{Mqt}(\omega_2/u)] \\ & - r_p PA \sin \eta_2\} \hat{j}_1 + \{(1/2)\rho Su^2 l [-C_{M\alpha}(v/u) \\ & + C_{M\alpha p}(pl/V_p)(w/u) + l C_{Mqt}(\omega_3/u)] \\ & - r_p PA \sin \eta_1 \cos \eta_2\} \hat{k}_1 \quad (41) \end{aligned}$$

The value of K_i ($i = 1,2,3,4,5,6$)⁴ get due to mechanical force and shockwave force are as given below

$$\begin{aligned} K_1 &= -\left[\frac{2g_X l}{u^2} - \varepsilon(2C_D - C_N) + 2Q + 2Q' - \varepsilon K_t^{-2} C_{Mqt}\right] \\ K_2 &= -\zeta \beta' + 2 \bar{\Omega}_X \\ K_3 &= -\varepsilon K_t^{-2} C_{M\alpha p} + \left(\frac{g_X l}{u^2}\right)^2 + \varepsilon^2 C_D (C_D - C_N) \\ & - \frac{g_X l}{u^2} \varepsilon(2C_D - C_N) + \zeta \beta' \bar{\Omega}_X - \bar{\Omega}_X^2 - \varepsilon K_t^{-2} C_{Mt} \\ & \left[\frac{g_X l}{u^2} - \varepsilon(C_D - C_N)\right] + (Q + Q') \left[\frac{2g_X l}{u^2} - \varepsilon(2C_D - C_N) \right. \\ & \left. - \varepsilon K_t^{-2} C_{Mqt}\right] + (Q + Q')^2 \\ K_4 &= \zeta \beta' \varepsilon(C_D - C_N) - \zeta \beta' \frac{g_X l}{u^2} - \\ & \bar{\Omega}_X \left[\varepsilon(2C_D - C_N) - \frac{2g_X l}{u^2} + \varepsilon K_t^{-2} C_{Mqt}\right] \\ & - (Q + Q') [\zeta \beta' - 2\bar{\Omega}_X] - \varepsilon K_t^{-2} C_{M\alpha p} \zeta \\ K_5 &= -\left\{\varepsilon(C_D - C_N) + \frac{g_X l}{u^2} + Q + Q' - \varepsilon K_t^{-2} \right. \\ & C_{Mqt} \left. \left[-\frac{l}{u^2} g_Y + M' PA \sin \eta_1 \cos \eta_2 + I\right] \right. \\ & \left. - (\zeta \beta' - \bar{\Omega}_X) \left(M' PA \sin \eta_2 - \frac{l}{u^2} g_Z\right) - \right. \\ & \left. K_t^{-2} \frac{r_p PA}{u^2 m} \sin \eta_1 \cos \eta_2\right\} \end{aligned}$$

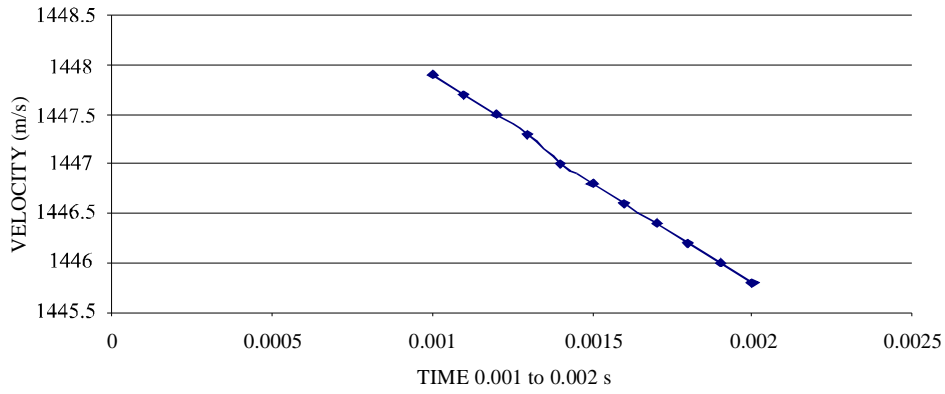


Figure 3. Reduction in velocity in the phase II.

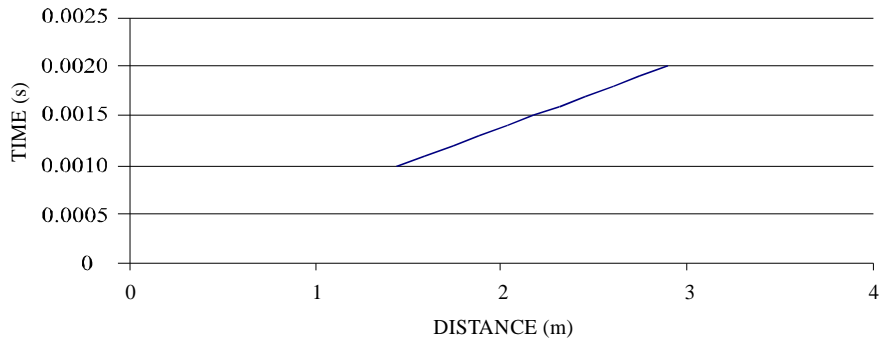


Figure 4. Distance against time.

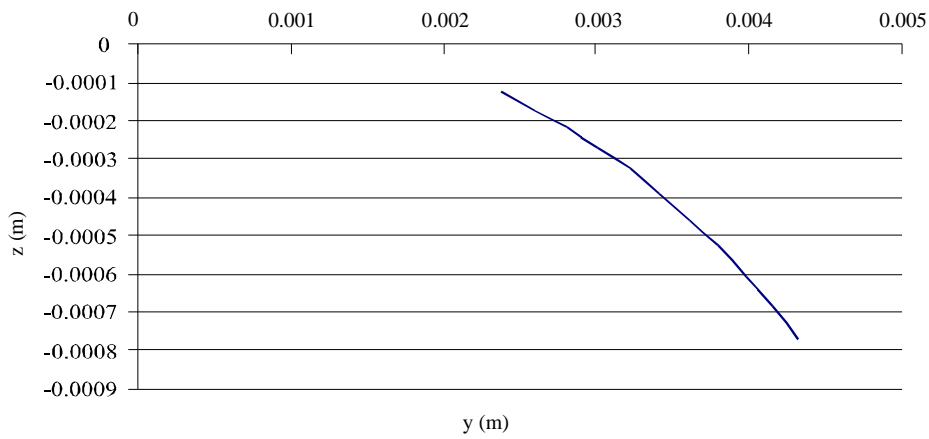


Figure 5. Cross plane motion.

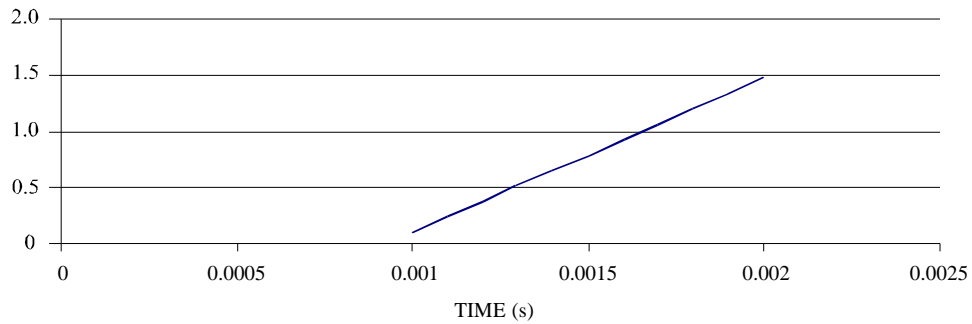


Figure 6. Increase in the angle of sabot and projectile during opening process.

$$K_6 = (\zeta\beta' - \overline{\Omega}_x) \left(-\frac{l}{u^2} g_Y + M'PA \sin \eta_1 \cos \eta_2 + I \right) + \left(\frac{g_X l}{u^2} - \varepsilon C_D + Q + Q' - \varepsilon K_t^{-2} C_{Mqt} \right) (M'PA \sin \eta_2 + \frac{l}{u^2} g_Z) + K_t^{-2} \frac{r_p PA}{u^2 m} \sin \eta_2 \quad (42)$$

Q consists of the terms due to propellant gas pressure, and Q' are the terms due to shockwave and mechanical force.

The modify stability parameter⁵ is defined as

$$S_M = 1 + \frac{(2K_4 / K_1) - K_2}{\sqrt{K_1^2 + K_2^2}} \quad (43)$$

where $0 < S_M < 2$ for the stable motion. It has been observed that the stability parameter $S = 1.859147$ gets modified to $S_M = 1.891418$ due to pressure and damping moment².

The value of stability parameter further gets modified to $S'_M = 1.89354021$ but it still lies between 0 to 2, which implies that the shock wave and mechanical forces does affect the stability of projectile during its motion in phase II.

7. VARIATION IN SEPARATION OF SABOTS

Consider that the sabots do not get separated simultaneously due to some unexpected variation during flight. That means the initial conditions for the sabots during their opening are different. All the three sabots start opening at three different time instances.

Let us consider one particular case where two sabots start opening at same instant of time ($t = 0.001$ s) and the third starts opening with a delay of 0.001 s ($t = 0.002$ s). The shock wave force and the mechanical force due to third sabot component opening will not be considered during this second phase of motion.

The scalar equations are

$$m \left(\frac{\partial u}{\partial t} + \omega_2 w - \omega_3 v \right) = PA \cos \eta_1 \cos \eta_2 - (1/2) \rho S u^2 C_D - 2K L_c \cos \theta_{3i} + (1/2) \rho V p \pi (D/3) L_s (Vp + L_c \dot{\theta}_{3i} \sin^2 \theta_{3i}) - mg \sin \theta_1 \quad (44)$$

$$\left(\frac{\partial v}{\partial t} + \omega_3 u - \omega_1 w \right) = -PA \sin \eta_1 \cos \eta_2 + (1/2) \rho S u^2 [-C_N (v/u) + l C_{Nqt} (\omega_3 / u)] - (1/2) K L_c \sin \theta_{3i} \cos \gamma_1 + (1/4) \rho V p \pi (D/3) L_s L_c \dot{\theta}_{3i} \sin \theta_{3i} \cos \theta_{3i} \cos \gamma_i - mg \cos \gamma_1 \cos \theta_1 \quad (45)$$

$$m \left(\frac{\partial w}{\partial t} + \omega_1 v - \omega_2 u \right) = PA \sin \eta_2 - (1/2) \rho S u^2 [(w/u) C_N + l C_{Nqt} (\omega_2 / u)] + (1/2) K L_c \sin \theta_{3i} \sin \gamma_1 - (1/4) \rho V p \pi (D/3) L_s L_c \dot{\theta}_{3i} \sin \theta_{3i} \cos \theta_{3i} \sin \gamma_i + mg \sin \gamma_1 \cos \theta_1 \quad (46)$$

The value of stability parameter gets modified from $S'_M = 1.89354021$ to $S''_M = 1.893548601$.

8. CONCLUSIONS

1. For an FSAPDS projectile, a mathematical model has been developed in second phase where the mechanical and shockwave forces act on the projectile due to sabot separation. The trajectory has been simulated. It is observed that the addition of the mechanical and shockwave actions in the simulation does not affect the trajectory of the projectile but initiates the sabot opening process.
2. The stability parameter increases due to opening of sabots but the projectile still remains in the stable zone.
3. Due to unequal separation of sabot the forces and moments acting on the projectile are asymmetric which makes the projectile instable compared to the case when simultaneous sabot opening takes place.

ACKNOWLEDGMENTS

The authors are grateful to the Director of the Defence Institute of Advanced Technology, the Chairman and Director of the P.E. Society's Modern College of Engineering and VIIT, Pune for their support and encouragement.

REFERENCES

1. Yang, Q.R. A study of dynamic modelling of sabot discard. *In Proceedings of the 12th International Symposium of Ballistics, USA, 1990*, pp. 69-78.
2. Acharya, R.S. & Naik, S.D. Perturbation of initial stability of a FSAPDS projectile, *Def. Sci. J.*, 2006, **56**(5), 753-68.
3. Beer, F.R. & Johnston Jr. *Vectors mechanics for engineers*, Tata McGraw Hill Publication, New Delhi, pp. 672-75.
4. Bakshi, S.B. & Sharma, K.C. A fresh look at the free dynamics of a spinning projectile. *Sadhana*, 1988, **12**(4), 321-37.
5. Naik, S.D. Stability criterion for a finned spinning projectile, *Def. Sci. J.*, 2000, **50**, 31-35.